frontiers | Frontiers in Agronomy

TYPE Original Research
PUBLISHED 06 January 2026
DOI 10.3389/fagro.2025.1697188

OPEN ACCESS

EDITED BY
Ali T. Mohammed,
University of Arizona, United States

REVIEWED BY
Ana Maria Tarquis,
Polytechnic University of Madrid, Spain
Koffi Djaman,
New Mexico State University, United States
Sahar Rezaei Koujani,
Drought School, United States

*CORRESPONDENCE
Tondani Sanah Ramabulana
ramabulana.sanah@edu.pte.hu

RECEIVED 01 September 2025
REVISED 28 November 2025
ACCEPTED 08 December 2025
PUBLISHED 06 January 2026

CITATION
Nxumalo GS, Ramabulana TS, Dlamini Z, Louis A and Nagy A (2026) Integrating OPTRAM and machine learning with multimodal EO proxies for optimized irrigation scheduling in smallholder systems: a Vhembe District case study. *Front. Agron.* 7:1697188. doi: 10.3389/fagro.2025.1697188

Integrating OPTRAM and machine learning with multimodal EO proxies for optimized irrigation scheduling in smallholder systems: a Vhembe District case study

Gift Siphiwe Nxumalo[1,2], Tondani Sanah Ramabulana[3]*, Zibuyile Dlamini[4], Angura Louis[1,2] and Attila Nagy[1,2]

[1]Institute of Water and Environmental Management, Faculty of Agricultural and Food Sciences and Environmental Management, University of Debrecen, Debrecen, Hungary, [2]National Laboratory for Water Science and Water Safety, Institute of Water and Environmental Management, Faculty of Agricultural and Food Sciences and Environmental Management, University of Debrecen, Debrecen, Hungary, [3]Institute of Geography and Earth Sciences, Faculty of Sciences, University of Pécs, Pécs, Hungary, [4]Doctoral School of Environmental Sciences, Institute of Environmental Sciences, Hungarian University of Agriculture and Life Sciences, Gödöllő, Hungary

Climate variability and recurrent droughts pose increasing irrigation challenges for smallholder maize farmers in southern Africa. This study developed a scalable Earth observation and artificial intelligence (EO–AI) framework combining satellite data, machine learning, and crop water modeling to estimate daily maize actual crop evapotranspiration (ETc) in South Africa's Vhembe District. Five machine learning models were rigorously validated against benchmark ET_c derived from the FAO-56 Penman–Monteith reference evapotranspiration (ET_0) method multiplied by locally calibrated crop coefficients (K_c). Random Forest and k-Nearest Neighbors models demonstrated superior performance, with R^2 consistently exceeding 0.99, root mean square error (RMSE) below 0.06 mm/day, and normalized RMSE (NRMSE) less than 2%, outperforming support vector machine, MARS, and XGBoost models. The EO–AI framework effectively captured fine-scale spatial and temporal ET_c variability, with daily actual maize ET_c at 6.5 mm/day during peak crop sensitivity periods. An operational irrigation decision-support prototype translated these predictions into targeted field-level water-deficit alerts for farmers. This work highlights the value of EO–AI frameworks for delivering high-resolution, daily ET_c mapping in fragmented, cloud-prone landscapes, enabling more precise and resilient irrigation strategies for smallholder systems.

KEYWORDS

artificial intelligence, crop water modeling, earth observation, evapotranspiration, irrigation, machine learning, smallholder maize farmers

1 Introduction

Climate change poses a major challenge to sustainable agriculture, particularly in water-scarce regions such as the Vhembe District in Limpopo, South Africa. This district relies largely on smallholder and subsistence farming, which is increasingly threatened by recurrent droughts, erratic rainfall, and rising temperatures. Maize (Zea mays), the staple crop for local livelihoods, is highly vulnerable to water stress. Water shortages during key growth stages—including germination, tillering, stem elongation, and tasselling—can significantly reduce yields (Ibrahim et al., 2016). Drought conditions, coupled with high evapotranspiration (ET) demand and low relative humidity, further exacerbate yield losses in dryland maize systems (Daryanto et al., 2016). These vulnerabilities are critical in arid and semi-arid environments, where nearly two billion people depend on agriculture for food security (El-Beltagy and Madkour, 2012). Rising temperatures amplify crop water requirements (Trout and DeJonge, 2021), highlighting the urgent need for efficient irrigation strategies.

Accurate estimation of actual crop evapotranspiration (ET_c)—which represents the water consumed by a specific crop under given field management and environmental conditions—is central to irrigation scheduling. ET_c is typically calculated as the product of reference evapotranspiration (ET_0, representing evapotranspiration from a standardized grass reference surface) and a crop-specific coefficient (K_c): $ET_c = K_c \times ET_0$. This approach enables agronomically sound irrigation management decisions by quantifying water requirements under specific soil and climatic conditions. ET_0 is commonly estimated using the FAO-56 Penman-Monteith equation (Allen et al., 1998), which integrates meteorological variables including solar radiation, air temperature, humidity, and wind speed. K_c adjusts ET_0 to account for crop-specific characteristics such as canopy development, stomatal resistance, and rooting depth, which vary across phenological stages. However, existing approaches face limitations in smallholder contexts. Direct methods such as lysimeters and eddy covariance systems provide high accuracy but are prohibitively expensive, costing above USD 50,000 and USD 20,000 respectively, and are unsuitable for fragmented farmlands (Cameira and Santos Pereira, 2019; Mauder et al., 2021). Empirical models like the Food and Agriculture Organization (FAO) Penman–Monteith method require dense meteorological inputs that are rarely available in rural Africa (Ford et al., 2015; Datta et al., 2018), while simplified models such as Hargreaves often overestimate ET_c in humid or advection-dominated climates (Aroonsrimorakot and Laiphrakpam, 2023).

Earth observation (EO)-based approaches, including the Surface Energy Balance Algorithm for Land (SEBAL), the Mapping EvapoTranspiration at high Resolution with Internalized Calibration (METRIC), and the Normalized Difference Vegetation Index (NDVI)-based crop coefficient (K_c) methods, offer wide spatial coverage but are strongly constrained by cloud cover (Pareeth and Karimi, 2023). In Vhembe, cloudiness exceeds 60% annually, severely limiting the reliability of optical-based ET_c estimates (Matasane and Kahn, 2025). This underscores the need for complementary EO data streams that combine multispectral data fusion to ensure both spatial accuracy and temporal consistency. At the same time, machine learning (ML) methods have demonstrated strong potential for ET_c modelling, achieving coefficients of determination (R^2) above 0.98 in controlled studies. However, their performance depends heavily on the availability of high-quality inputs and local calibration, which remain scarce in sub-Saharan Africa (Ali et al., 2015).

This study develops a scalable Earth Observation–Artificial Intelligence (EO–AI) framework that integrates optical data from Sentinel-2 and Moderate Resolution Imaging Spectroradiometer (MODIS) to mitigate cloud cover limitations, coupled with the Optical Trapezoid Model (OPTRAM) for evapotranspiration estimation. The framework is calibrated and validated using local meteorological records, *in situ* soil moisture measurements from Agricultural Research Council (ARC) probes (0–100 cm depth), and benchmarked against FAO-56 Penman–Monteith-derived actual crop evapotranspiration (ETc,FAO-56).K_c values were aligned with maize phenological stages following the Biologische Bundesanstalt, Bundessortenamt, and CHemische Industrie (BBCH) scale to ensure phenology- based accuracy.

The novelty of this study lies in combining EO data and AI to deliver agronomically relevant irrigation insights for smallholder maize farmers. The specific objectives are:

(a) to develop an integrated ET_c modelling framework combining OPTRAM, Sentinel-2 red-edge bands, and land surface temperature proxies calibrated against ARC soil moisture probes and phenology-aligned Kc values; (b) to generate a high-resolution, cloud-resilient vegetation index product through Sentinel-2 and the MODIS fusion for improved ET_c estimation; (c) to evaluate and compare ML algorithms—k-nearest neighbors (KNN), random forest (RF), support vector machines (SVM), multivariate adaptive regression splines (MARS), and extreme gradient boosting (XGB)—for ET_c prediction using statistical performance metrics and uncertainty analysis; (d) to benchmark EO–AI-derived ET_c estimates against FAO-56 approach actual crop evapotranspiration (ET_c,FAO-56 = $K_c \times ET_0$,PM) and *in-situ* soil moisture-derived Kc; and (e) to operationalize a precision irrigation advisory system that translates ET_c outputs into farmer-ready, field-specific irrigation recommendations.

By delivering field-scale, actionable water-use insights without reliance on expensive ground sensors, this framework offers a practical and adoptable solution for precision irrigation in heterogeneous smallholder landscapes. It addresses key barriers of cost, infrastructure, and usability, while advancing AI-driven irrigation technologies that are scalable, context-aware, and tailored to the needs of southern African farmers (Babaeian et al., 2019; Ford and Quiring, 2019; Kolady et al., 2021).

2 Materials and methods

2.1 Study area

The Vhembe District, located in Limpopo Province, northern South Africa (22.1°–23.3°S, 29.5°–31.3°E), spans ~12,500 km²

within a semi-arid to sub-humid climate. Elevations range from ~200 m in river valleys to ~1,800 m in the Soutpansberg Mountains, producing strong gradients in rainfall, temperature, and soil water availability. Annual rainfall (400–800 mm) is concentrated in summer but is highly variable, with recurring droughts, short floods, and evapotranspiration exceeding precipitation (Shikwambana et al., 2021).

Smallholder mixed crop–livestock systems dominate land use. Maize and sorghum are staple crops, complemented by beans, groundnuts, and vegetables, while cattle, goats, and poultry diversify livelihoods (Maponya, 2021). Soils are primarily ferralsols, ferrosols, and luvisols, moderately fertile but prone to nutrient depletion. Remote sensing indicates ongoing conversion of rangelands to cropland and settlements, affecting ecosystem resilience (Nuwarinda et al., 2022).

Hydrologically, the district depends on transboundary rivers—including the Limpopo and Luvuvhu (Figure 1)—as well as groundwater resources, which are currently experiencing decline. The Soutpansberg Mountains generate orographic rainfall and support biodiversity and culturally significant medicinal plants, vital to Venda and Bapedi communities (Semenya and Potgieter, 2014). Despite socioeconomic challenges, the district combines indigenous knowledge and emerging practices, including conservation agriculture and small-scale irrigation, increasingly supported by satellite-based monitoring to enhance resilience and food security (Maponya, 2021).

2.2 Framework of the study

2.2.1 Data sources and description

Satellite Data: Sentinel-2 Multispectral Instrument (MSI) imagery was used to derive vegetation indices— NDVI and Fractional Vegetation Cover (FVC)—as well as broadband albedo and Land Surface Temperature (LST). MODIS NDVI composites from the MOD13A1 product with 250 m spatial resolution were derived. A Shuttle Radar Topography Mission (SRTM) 30 m Digital Elevation Model (DEM) provided topographic correction and terrain-based parameterization (Figure 2).

Ground Data: Meteorological observations (temperature, relative humidity, wind speed, radiation, rainfall) were obtained from the South African Weather Service (SAWS) (Figure 1). Soil moisture (volumetric water content in mm/dm, 0, 20, 40, 60, 80, 100 cm depth) was accessed from Agricultural Research Council (ARC) field stations for calibration and validation (Moeletsi et al., 2022).

2.2.2 Workflow overview

The workflow integrates Earth Observation (EO) data, the Optical Trapezoid Model (OPTRAM), and machine learning (ML) to estimate actual crop evapotranspiration (ET_c) (Figure 2).

Step 1: EO data preprocessing and Data fusion

Sentinel-2 images were atmospherically corrected and co-registered. To produce cloud-resilient NDVI composites, Sentinel-2 NDVI (NDVI = (NIR – Red)/(NIR + Red)) with<20% cloud

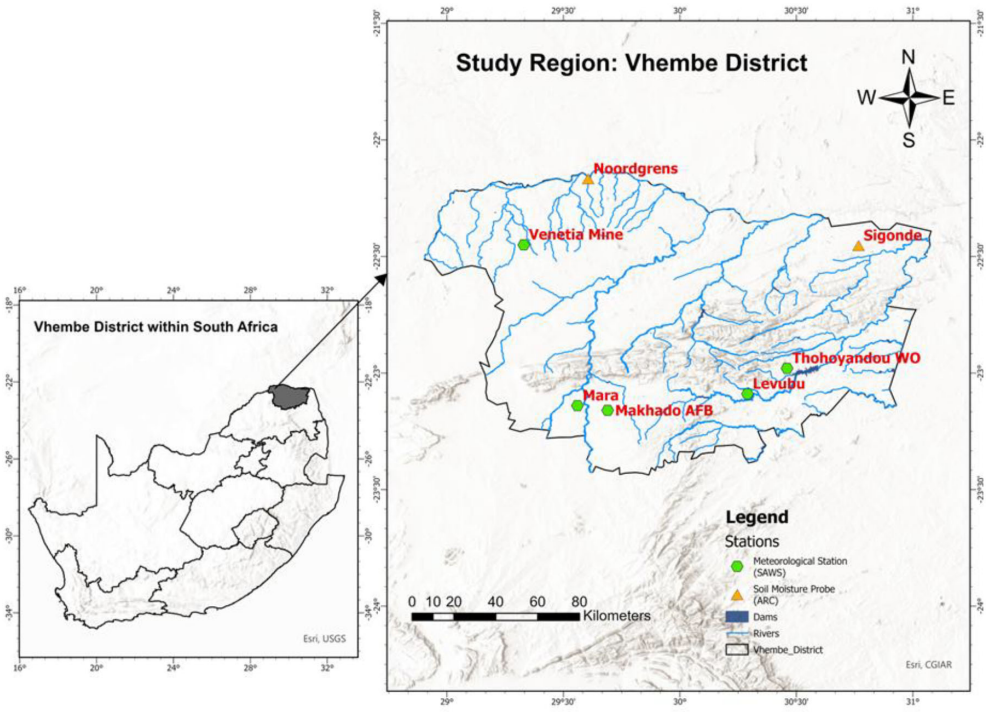

FIGURE 1
Spatial overview of the Vhembe District study region, South Africa.

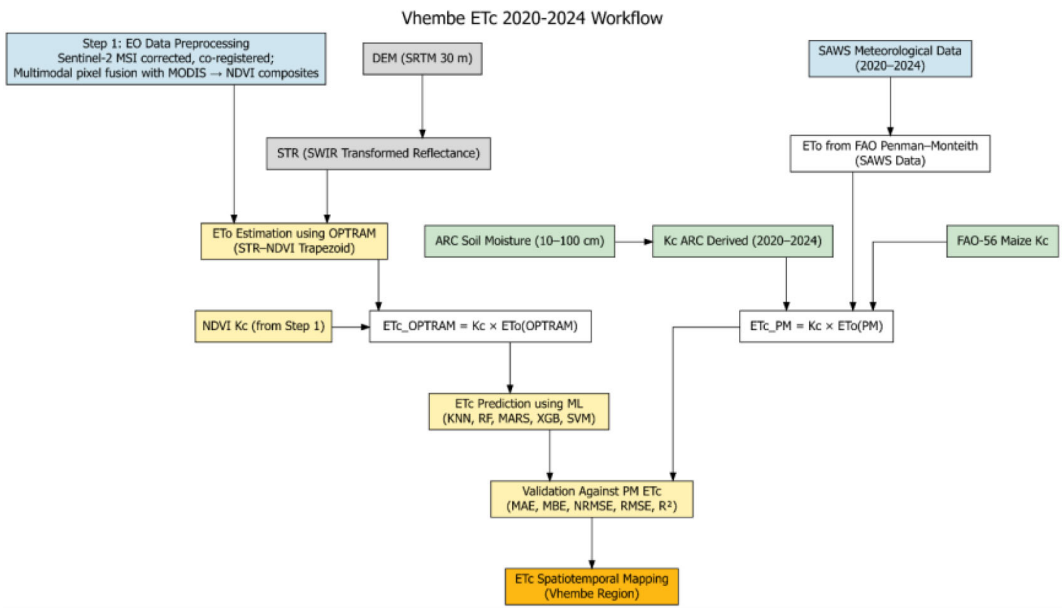

FIGURE 2
Vhembe District ET_c Workflow: 2020–2024.

coverage was prioritized. Missing pixels were filled with MODIS NDVI (MOD13A1), and persistent gaps were assigned a fallback value (NDVI = 0.10).

A linear fusion approach generated a continuous NDVI time series, subsequently converted to basal crop coefficient (K_{cb}, representing crop transpiration under well-watered conditions without soil evaporation) (Allen et al., 1998; (Siphiwe et al., 2024) using:

$$K_{cb} = a \cdot NDVI_{fused} + b$$

where a=1.20 and b=0.20, calibrated against ARC soil moisture and maize phenology data. For irrigated maize under the management conditions observed in Vhembe District, where soil surface is largely shaded during mid- and late-season stages and evaporation is minimal, K_{cb} approximates the single K_c. Therefore, K_{cb} values were used as K_c in subsequent actual ET_c calculations: $ET_c = K_c \times ET_0$. The full methodology for data fusion is detailed in Supplementary Material Table A1.

Step 2: Crop coefficient (K_c) estimation

1. NDVI–K_{cb} regression was applied to estimate basal crop coefficients for maize and other crops, linking vegetation dynamics to crop transpiration (the primary component of crop water use under irrigated conditions (Aidoo et al., 2021; Costa et al., 2023; Nagy et al., 2024). These K_{cb} values were subsequently used as single K_c values for ET_c calculation given the well-managed irrigation conditions and canopy coverage in the study area and given that soil water evaporation may be negligible but not null.

Step 3: OPTRAM-Based Evaporative Fraction and Actual Crop Evapotranspiration (ETc) Estimation

The Optical Trapezoid Model (OPTRAM) was used to estimate pixel-wise evaporative fraction (EF) (see Equation 1) from NDVI–LST space (Ambrosone et al., 2020):

• Wet and dry endmembers were identified per pixel using fused NDVI percentiles (T_{wet}: 5th percentile LST at high NDVI, T_{dry}: 95th percentile LST at low NDVI).

Evaporative fraction:

$$EF = T_{dry} - T_{wet} / (T_{dry} - T_{pixel}) \quad (1)$$

clipped to maintain physical consistency. OPTRAM-derived EF was combined with MODIS PET (MOD16A2, scaled to mm day^{-1}) (Becaro Crioni et al., 2025) to compute ETo_{OPTRAM} (reference evapotranspiration from OPTRAM then multiplied by K_c to yield spatially explicit ET_c (Equation 2):

$$ETo_{OPTRAM} = EFx\ PETMODIS \quad (2a)$$

$$ETcOPTRAM = Kc\,.\,ETo_{OPTRAM} \quad (2b)$$

A 500 m smoothing kernel minimized pixel-level noise. Local calibration of OPTRAM parameters was performed by fitting the wet and dry edges within the NDVI–STR feature space using linear regression on multi-date Sentinel-2 imagery (Quintana-Molina et al., 2023). This calibration utilized ground-truth soil moisture data from ARC probes alongside maize phenology information to tailor the model parameters—specifically, the slopes and intercepts of wet and dry edges—to the local soil and vegetation conditions (Mohamadzadeh et al., 2025). This site-specific fitting ensures accurate estimation of the evaporative fraction and spatially explicit evapotranspiration (ETc), as further detailed in Supplementary Material Table A1.

Step 3a: Benchmark ET_c Calculation Using FAO-56 Approach

To validate the OPTRAM-derived ETc estimates, benchmark actual crop evapotranspiration values (ETc,FAO-56) were computed following the standard FAO-56 dual-source approach (Allen et al., 1998):

$$ET_c, FAO-56 = K_c \times ET_0, PM \quad (3)$$

where ET_0,PM is the FAO-56 Penman-Monteith reference evapotranspiration, calculated using Equation 4:

$$ET_0, PM = [0.408\Delta(Rn - G) + \gamma(900/(T + 273))u_2(es - ea)]/[\Delta + \gamma(1 + 0.34u_2)] \quad (4)$$

where:

Δ = slope of saturation vapor pressure curve (kPa °C^{-1})

Rn = net radiation at crop surface (MJ m^{-2} day^{-1})

G = soil heat flux density (MJ m^{-2} day^{-1})

γ = psychrometric constant (kPa °C^{-1})

T = mean daily air temperature at 2 m height (°C)

u_2 = wind speed at 2 m height (m s^{-1})

es = saturation vapor pressure (kPa)

ea = actual vapor pressure (kPa)

Meteorological data for ET_0 calculation were obtained from five South African Weather Service (SAWS) stations across Vhembe District (Levubu, Makhado Air Force Base, Mara, Thohoyandou WO, Venetia Mine) (Figure 1). Missing data were gap-filled using inverse distance weighting from neighboring stations.

Standard FAO-56 crop coefficient values for grain maize under sub-humid climatic conditions ($RH_{min} \approx 45\%$, $u_2 \approx 2$ m/s) (Allen et al., 1998, Table 12) were used as initial reference values. These reference K_c values were adjusted for local Vhembe conditions using Equation 5:

$$K_{c,adj} = K_{c,tab} + 0.04(u_2 - 2) - 0.004(RH_{min} - 45)^{0.3} \quad (5)$$

where h = mean plant height during mid-season (2.0 m for maize). Further calibration was performed using ARC soil moisture observations and NDVI-derived K_{cb} values to capture local cultivar characteristics and evaporative demand.

Step 4: Machine learning modelling

Machine learning models were implemented to predict spatially continuous maize ET_c across the Vhembe District using R (v4.3.3). Five algorithms were tested: Random Forest (RF), k-Nearest Neighbors (KNN), Support Vector Machines (SVM with radial kernel), Multivariate Adaptive Regression Splines (MARS), and Extreme Gradient Boosting (XGB) (See Table 1). Input variables consisted of OPTRAM-derived ET_c raster values combined with geospatial coordinates (longitude and latitude), while the target variable was ETc,FAO-56 (Equation 3) derived from meteorological stations. The dataset was constructed via stratified random sampling (~10,000 points per year, 2020–2024) and split into 70% training and 30% testing subsets, ensuring no spatial or temporal overlap between sets to prevent data leakage (Zhu et al., 2023). Hyperparameter tuning (Table 2) was performed through 3-fold cross-validation or grid search within the training data to identify optimal model configurations and minimize overfitting (Sanchez et al., 2021). Model performance was then evaluated on the independent test set using multiple statistical metrics described in Section 2.4.

Step 5: Validation and mapping

ET_c predictions were validated against FAO-56 Penman–Monteith-derived actual crop evapotranspiration (ETc,FAO-56) (Allen, 2000) and ARC probes. Six metrics were computed: R^2, RMSE, NRMSE, MAE, MBE, and MSE. Confidence intervals (95%) were estimated via bootstrap resampling to quantify uncertainty.

2.4 Statistical evaluation analysis

Model validation employed multiple widely used statistical indices (As shown in Equations 6-11) to assess the accuracy and reliability of ML-predicted actual crop evapotranspiration (ET_c,ML) relative to FAO-56 approach (Equation 3)

(Filgueiras et al., 2019). These metrics included Mean Absolute Error (MAE), Mean Bias Error (MBE), Root Mean Square Error (RMSE), Normalized RMSE (NRMSE), Mean Squared Error (MSE), and the coefficient of determination (R^2).

MAE quantified the average magnitude of prediction errors, providing a direct measure of overall model accuracy (Willmott and Matsuura, 2005), while MBE indicated systematic over- or underestimation, which is critical for irrigation planning (Moriasi et al., 2007). RMSE emphasized larger deviations that could impact water balance during peak crop demand (Legates and McCabe,

TABLE 1 Key machine learning methods for estimating maize evapotranspiration (ET_c): representative equations and foundational references.

#ML method	Representative equation	Citation
k-Nearest Neighbors (KNN)	$\hat{y} = \frac{1}{k}\sum_{i=1}^{T} y_i$	(Cover and Hart, 1967)
Random Forest (RF)	$\hat{y} = \frac{1}{T}\sum_{t=1}^{T} h_t(x)$	(Breiman, 2001)
MARS (Multivariate Adaptive Regression Splines)	$f(x) = \sum_{m=1}^{M} c_m \ B_m(x)$	(Friedman, 1991)
Gradient Boosting Machine (GBM/XGB)	$f(x) = F_{m-1}(x) + \nu \ h_m(x)$	(Friedman, 2001)
Support Vector Machine (SVM)	$f(x) = \sum_{i=1}^{N} \alpha_i y_i K(x_i, x) + b, \quad K(x_i, x) = exp(-\|x_i - x\|^2)$	(Cortes and Vapnik, 1995)

TABLE 2 Machine learning hyper-parameterization and training.

Model	Input features	Preprocessing	Hyperparameter optimization	Notes
KNN	OPTRAM ET_c from rasters (Longitude, Latitude as coordinates)	Missing values removed	tuneLength = 3 via 3-fold cross-validation on training data	Baseline distance-based model; uses spatial proximity for ET_c prediction
Random Forest (RF)	OPTRAM ET_c from rasters (Longitude, Latitude)	Missing values removed	mtry = max(1, floor(sqrt(2))), splitrule="variance", min.node.size=5, num.trees = 200 (fixed)	Ensemble tree-based; robust to outliers and noise; captures complex ET_c relationships
SVM (RBF kernel)	OPTRAM ET_c rasters (Longitude, Latitude)	Missing values removed, centered and scaled to mean=0, SD=1	tuneLength = 3 via 3-fold cross-validation on training data	Flexible nonlinear regression model for ET_c spatial variability
MARS (Earth)	OPTRAM ET_c rasters (Longitude, Latitude)	Missing values removed, numeric scaling	tuneLength = 3 via 3-fold cross-validation on training data	Piecewise linear regression capturing complex ET_c patterns
XGBoost (XGB)	OPTRAM ET_c rasters (Longitude, Latitude)	Missing values removed	tuneLength = 3 via 3-fold cross-validation on training data	Gradient boosting; strong performance and regularization on ET_c prediction

All models used OPTRAM ETc raster values with longitude and latitude as predictors to validate OPTRAM ETc against FAO Penman–Monteith ET_c (ET_c PM). Data were split 70/30 for training and independent testing. Missing values were removed for all models; SVM was additionally centered and scaled. Hyperparameters were tuned via 3-fold cross-validation (KNN, SVM, MARS, XGBoost) or a fixed grid (Random Forest). Final evaluation was performed on the testing set to assess predictive performance.

1999), and NRMSE allowed standardized error comparison across varying ET_c magnitudes (Mentaschi et al., 2013). R^2 reflected the proportion of variance in observed ETc explained by the ML models, with higher values indicating strong temporal and spatial reproducibility (Reusser et al., 2009).

$$R^2 = 1 - \frac{\sum_{i=1}^{n}(y_i - \acute{y}_i)^2}{\sum_{i=1}^{n}(y_i - \bar{y})^2} \quad (6)$$

$$RMSE = \sqrt{\frac{\sum_{i=1}^{n}(y_i - \acute{y}_i)^2}{n}} \quad (7)$$

$$NRMSE = \frac{\sqrt{\frac{\sum_{i=1}^{n}(y_i - \acute{y}_i)^2}{n}}}{(\bar{y})} \quad (8)$$

$$MSE = \frac{1}{n}\sum_{i=1}^{n}(y_i - \acute{y}_i)^2 \quad (9)$$

$$MAE = \frac{1}{n}\sum_{i=1}^{n}|y_i - \acute{y}_i| \quad (10)$$

$$MBE = \frac{1}{n}\sum_{i=1}^{n}(y_i - \acute{y}_i) \quad (11)$$

Where: y_i, $\acute{y}_i$ are observed and predicted ET_c (mm day^{-1}), respectively; $\bar{y}$ is the mean observed ET_c; n is the number of validation samples. These complementary metrics collectively provided a rigorous framework for evaluating both the statistical robustness and agronomic reliability of the ML models for smallholder maize irrigation management.

2.7 Software & tools

Sentinel-2 and MODIS imagery were accessed and preprocessed in Google Earth Engine (GEE), including atmospheric correction, cloud masking, and compositing. Further processing, temporal aggregation, and raster alignment were performed in R and ArcGIS. Machine learning modeling for ET_c prediction was implemented in R using XGBoost, scikit-learn (via reticulate), and TensorFlow. Spatial analyses, including raster operations and zonal statistics, and all visualizations were conducted in ArcGIS and R.

3 Results

3.1 Climatic variability

Figure 3 presents a climograph for the Vhembe maize growing seasons across four years (2020/21 to 2023/24), highlighting monthly changes in humidity (%), rainfall (mm), temperature (°C), and wind speed (m/s) during the November to March period. Distinct crop growth stages—emergence, vegetative, flowering, grain filling, and maturity—are indicated with coloured bands, directly linking meteorological shifts to critical phases of crop development.

- Humidity and rainfall show synchronized peaks, especially in December to March, which coincide with key stages such as flowering and grain filling. Years with higher cumulative rainfall (2020/21, 2022/23) align with superior moisture conditions for optimal maize growth and grain set.
- Temperature trends reveal several late-summer months where maximum values approach or exceed thresholds (>35°C) known to increase evaporative demand and potential crop stress, particularly when compounded by periods of low humidity.
- Wind speed fluctuations, although less pronounced, overlap with dry spells and further elevate moisture loss risk.

By visualizing these meteorological variables alongside crop stages, Figure 3 illustrates specific windows of vulnerability and opportunity for targeted irrigation intervention. These insights

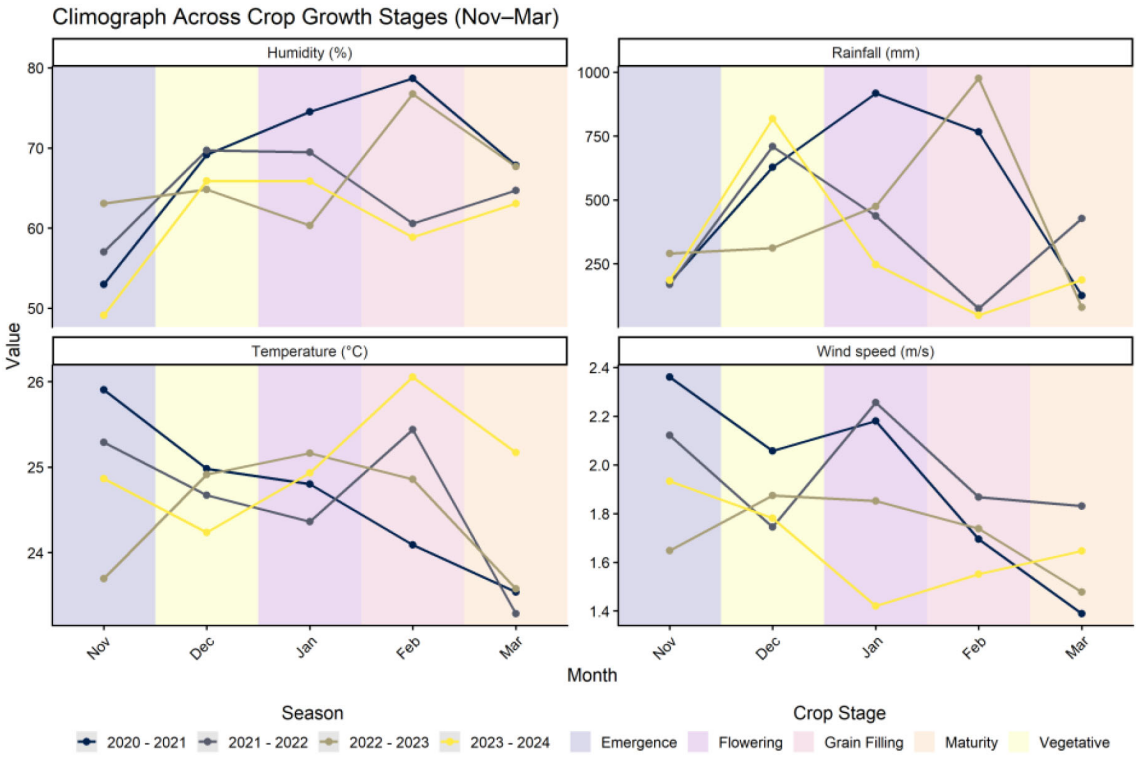

FIGURE 3
Seasonal weather trends and crop phenological stages (Nov–Mar, 2020–2024): interannual patterns of humidity, rainfall, temperature, and wind in relation to crop development.

underline the need for climate-responsive irrigation scheduling, especially for smallholder farmers facing variable seasonal rainfall and temperature extremes.

3.2 Maize K_c dynamics

The single crop coefficient trajectories reveal distinct seasonal shifts in maize water requirements, with locally calibrated K_c values exhibiting sharper increases and declines during crop development stages compared to the steadily rising FAO-56 reference coefficients (Figure 4). These calibrated values, derived from *in situ* soil moisture and phenological data, capture dynamic crop responses to local soil and climate variability. This enhanced temporal resolution enables more precise daily evapotranspiration estimation and facilitates fine-tuned irrigation scheduling, particularly during critical yield-sensitive phases such as silking and grain filling. The alignment of K_c peaks with shaded phenological periods underscores the importance of using dynamic, place-specific crop coefficients in managing maize water use.

3.2.1 FAO-56 reference and site-calibrated crop coefficients

The comparison between FAO-56 standard crop coefficients and site-calibrated values reveals important adaptations to local Vhembe conditions (Table 3). Site-calibrated Kc values were approximately 4–13% higher than the FAO-56 reference values during the mid-season stage, while during the grain-filling stage they were slightly lower, by about 6–8%, compared to FAO-56 values. This reflects higher evaporative demand driven by elevated vapor pressure deficit (VPD), local cultivar traits adapted to semi-arid conditions, and some intensive irrigation management practices observed in the study area.

The elevated mid-season Kc values (1.25–1.35 vs. FAO-56: 1.20) are attributable to three factors: (i) higher mean daytime vapor pressure deficit (VPD = 2.8–3.5 kPa) compared to FAO-56 reference conditions (VPD ≈ 2.0 kPa), which increases transpiration rates; (ii) local maize cultivars with deeper rooting systems (80–100 cm effective depth vs. FAO-56 assumed 60–80 cm) enabling sustained high transpiration even under moderate soil water depletion; and (iii) frequent irrigation scheduling (5–7 day intervals) maintaining soil moisture above 60% of field capacity throughout reproductive stages.

Phenological stage durations aligned well with the BBCH decimal growth scale, with total growing season length ranging from 135–165 days depending on planting date and cultivar maturity class. The vegetative development period (BBCH 20–39) was particularly sensitive to early-season water stress, with K_c rising rapidly from 0.35 to 1.30 over 35–40 days—a steeper trajectory than FAO-56 standard curves, reflecting rapid canopy expansion under favorable growing conditions.

The late-season decline in K_c (from 1.20 to 0.55) occurred more gradually than FAO-56 predictions, likely due to delayed senescence

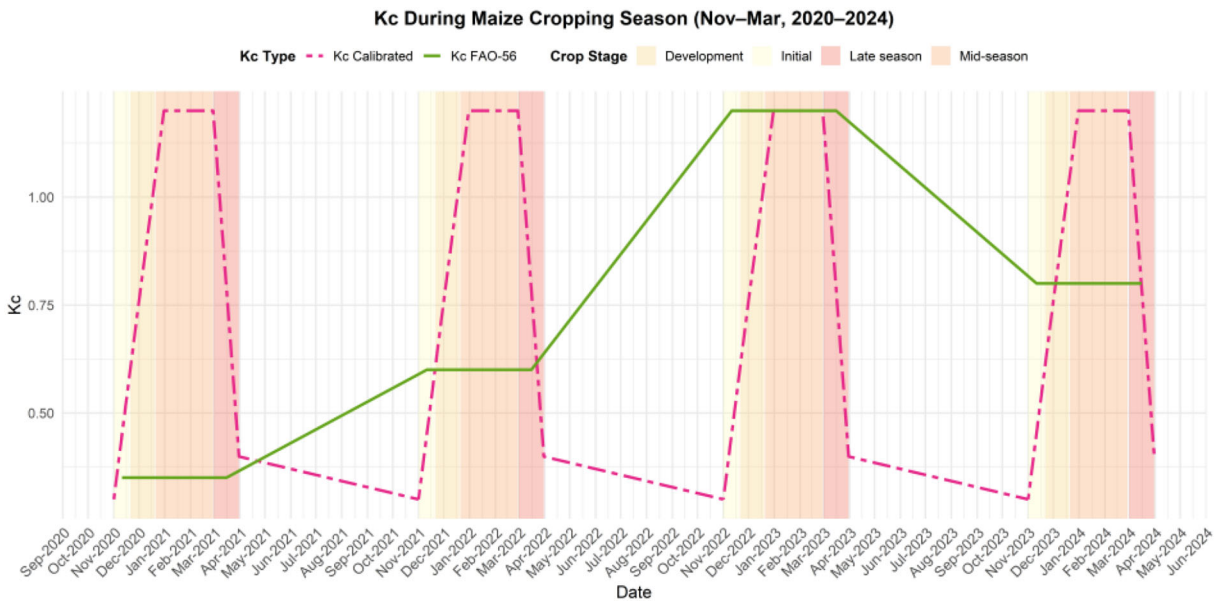

FIGURE 4
Temporal dynamics of maize single crop coefficient (K_c) throughout the cropping seasons (Nov–Mar, 2020–2024) in Vhembe, showing FAO-56 tabulated reference Kc values and site-calibrated K_c values derived from NDVI-based K_{cb} estimation across key phenological stages.

under irrigated conditions and the retention of functional green leaf area during grain maturation. This prolonged water use during grain filling (BBCH 70–79) has direct implications for irrigation cutoff timing: premature cessation of irrigation 2–3 weeks before harvest can reduce kernel weight by 8–12%, highlighting the value of site-specific K_c calibration for maximizing yield under water-limited conditions.

3.3 Seasonal patterns of maize crop evapotranspiration across sites

Seasonal mean maize actual crop evapotranspiration (ETc, FAO-56), estimated using the FAO-56 Penman-Monteith approach ($ET_c = K_c \times ET_0$,PM) and site-specific crop coefficients, exhibited strong variation across four stages (emergence, development, mid-season, late season) and five locations (Levubu, Makhado Air Force Base, Mara, Thohoyandou WO, Venetia Mine) over the 2020/21 to 2023/24 seasons (Figure 5). Across all years and sites, the mid-season consistently showed the highest ETc, highlighting this period as the primary window of water demand that determines final yield. The development and late-season stages displayed intermediate ETc values, while the emergence stage had the lowest water use.

Interannual and site-to-site ETc differences were evident, with locations such as Levubu and Venetia Mine generally requiring higher mid-season water inputs. These findings reflect both climatic variability and local management factors, underscoring the importance of targeted irrigation during periods of peak crop water use.

The results suggest that efficiently allocating water resources during the mid-season, supported by responsive advisory services and infrastructure, could enhance maize productivity and improve water use efficiency for smallholder farmers. Local adaptation of irrigation schedules, institutional support for extension, and improved farmer access to seasonal ET_c forecasts are key for translating these findings into increased resilience and productivity at the community level.

TABLE 3 Phenological stage duration and crop coefficients.

Growth stage	Duration (days)	FAO-56 K_c	Site-calibrated K_c range	BBCH scale
Emergence (Initial)	20–25	0.30	0.28–0.35	00–19
Vegetative Development	35–40	0.30 → 1.20	0.35 → 1.30	20–39
Flowering & Silking (Mid)	40–50	1.20	1.25–1.35	60–69
Grain Filling	25–30	1.20 → 0.90	1.20 → 0.95	70–79
Maturity (Late)	15–20	0.90 → 0.60	0.85 → 0.55	80–99
Total Season	135–165	—	—	00–99

TABLE 4 Proposed multi-scenario planting-window framework for improving ET_c modelling in heterogeneous smallholder systems.

Scenario	Planting window	Total season (days)	Silking date range	Harvest window
Early	Nov 1–15	145–155	Dec 28–Jan 10	Mar 20–30
Standard	Nov 16–30	135–145	Jan 8–20	Mar 25–Apr 5
Late	Dec 1–15	125–135	Jan 18–30	Apr 1–12

3.4 OPTRAM ETc estimation

Spatial maps of daily mean maize actual evapotranspiration (ET_c), generated using the OPTRAM model for Vhembe from 2020 to 2024, reveal persistent and pronounced differences in crop water demand across the region (Figure 6). Across all years, northern and central zones consistently exhibited high ET_c values, indicating elevated evaporative demand and increased irrigation requirements relative to southern and southeastern areas, where lower ET_c prevailed. Notably, interannual variability amplified spatial disparities during drier years, accentuating the risk of localized soil moisture deficits and yield instability in high-ET_c zones.

The practical significance of these findings lies in their immediate utility for smallholder irrigation targeting. By identifying fields located within ET_c hotspots, farmers and extension agents can prioritize water delivery during critical growth periods, reducing crop stress and optimizing returns on limited irrigation resources. Furthermore, the recurring spatial patterns support institutional planning—policy makers and farmer cooperatives can use ET_c maps to guide infrastructure investment, drought contingency initiatives, and equitable distribution of technical support.

For smallholder farmers, adopting spatially informed irrigation scheduling based on ET_c mapping allows a move away from uniform watering practices toward tailored, site-specific strategies. This shift directly enhances climate resilience, conserves water resources, and promotes sustainable intensification in vulnerable landscapes.

3.5 Machine learning maize ETc predictions

Spatial predictions of daily maize actual crop evapotranspiration (ET_c) in the Vhembe District (Figures 7A–E) reveal distinct interannual and geographic variation in water requirements from 2020 to 2024. Notably, in 2021 (Figure 7B), southeastern and central regions exhibit daily actual ET_c of 6.5 mm during critical reproductive growth and grain filling stages, corroborated by K_c profiles (Figure 4, calibrated K_C graph).

The machine learning models KNN and RF consistently deliver the most accurate ET_c predictions, with RMSE values between 0.039 and 0.060 mm/day and very high R^2 values (>0.99 for KNN and around 0.99 for RF) across years, indicating excellent fit and low error margins. These metrics demonstrate agronomically

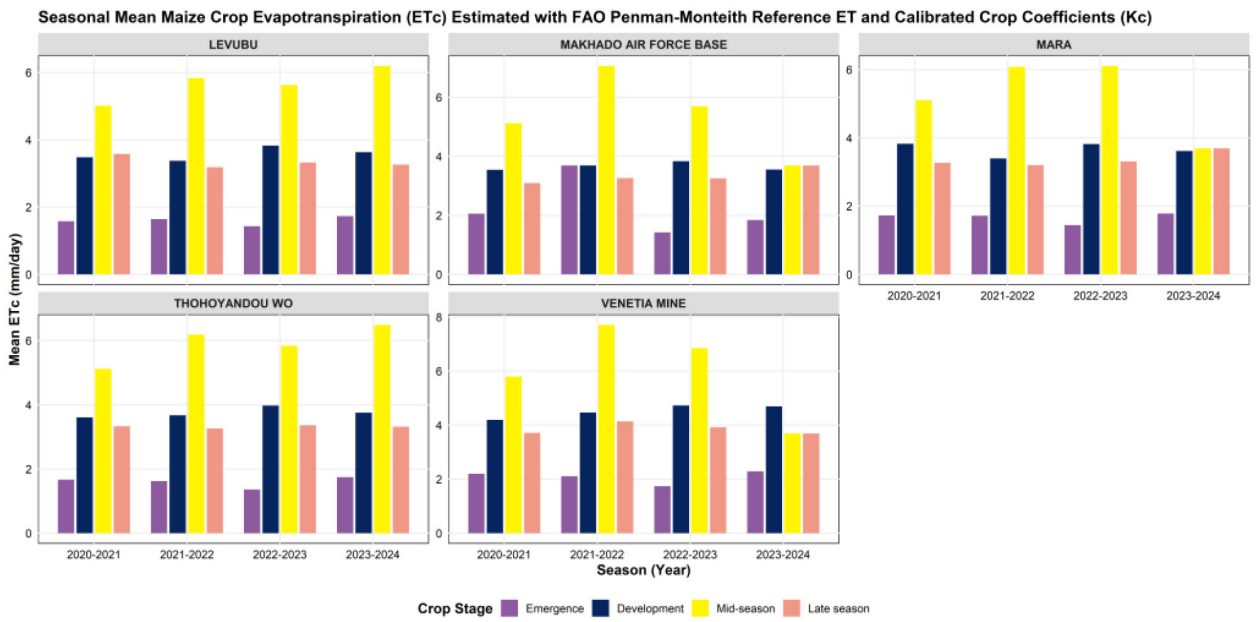

FIGURE 5
Seasonal mean maize actual crop evapotranspiration (ET_c) by growth stage and site (2020/21–2023/24), estimated using FAO-56 penman-monteith approach (ET_c,FAO-56 = K_c × ET_0,PM) with calibrated crop coefficients (K_c).

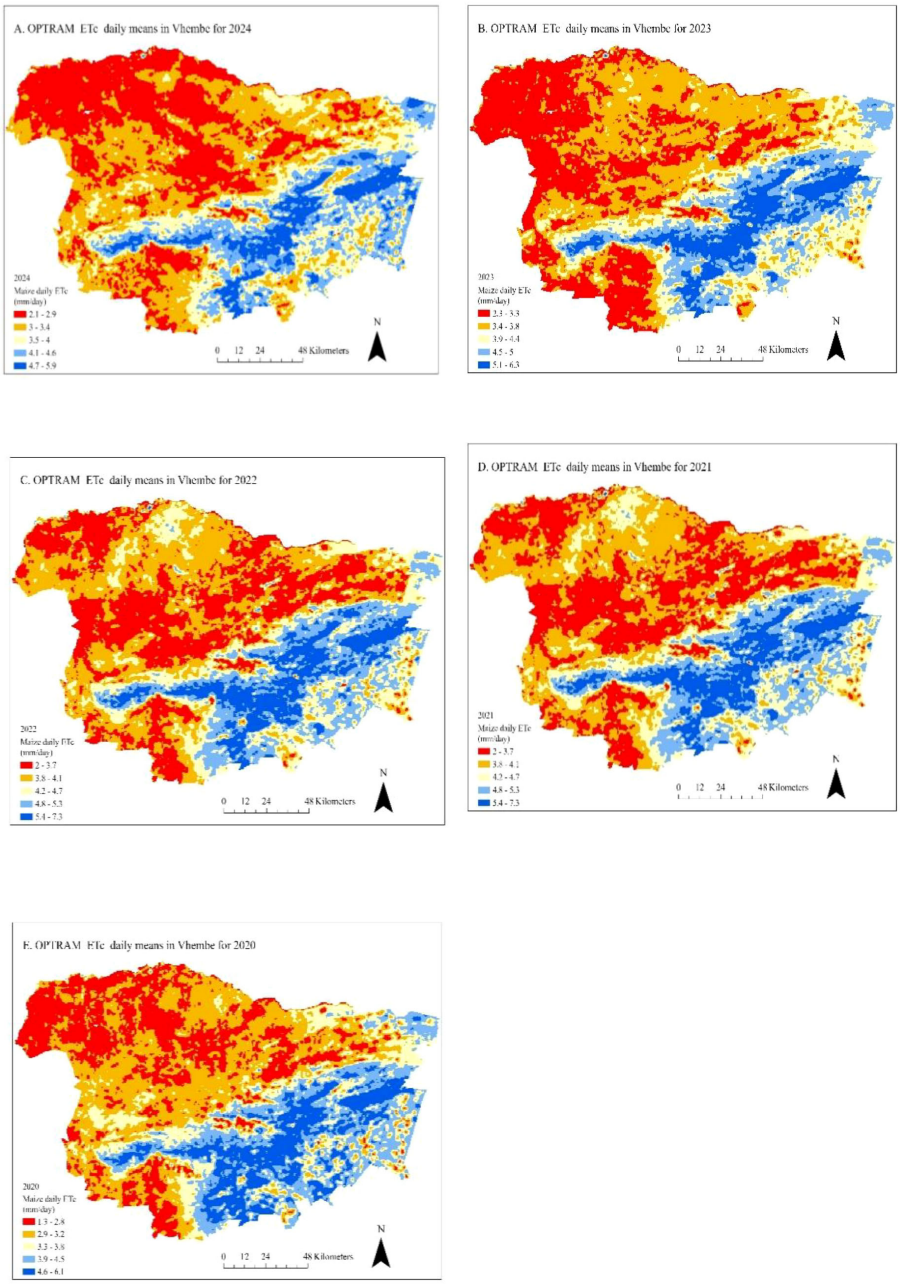

FIGURE 6
Annual spatial distribution of daily mean maize evapotranspiration (ET_c, mm/day) in Vhembe District, by Year: **(A)** 2024, **(B)** 2023, **(C)** 2022, **(D)** 2021, and **(E)** 2020, Estimated Using the OPTRAM Model.

meaningful accuracy, enabling precise irrigation scheduling during critical maize growth stages—such as silking and grain filling—when water demand peaks and crops are most sensitive to water stress, thereby maximizing yield potential.

Conversely, models such as SVM, MARS, and XGBoost show weaker predictive performance: R^2 values frequently below 0.75 and RMSE values up to ~0.42 mm/day undermine their ability to capture localized ET_c variability, limiting their effectiveness for precision irrigation during drought-sensitive periods.

Ensemble tree-based models (RF and KNN) effectively capture fine-scale spatial ET_c gradients and changing hotspots of water demand. This fidelity validates their deployment in operational irrigation advisory tools tailored for smallholder contexts. These models enable nuanced, site-specific water management decisions where farmers, guided by extension agents, can prioritize irrigation on high-demand fields while conserving water elsewhere, boosting irrigation efficiency and reducing risk.

In drought or variable climate years, these predictive insights facilitate early warning systems and contingency planning, strengthening farm-level resilience and sustainability. The integration of robust ML-driven spatial ETc maps with crop growth data represents a practical decision-support

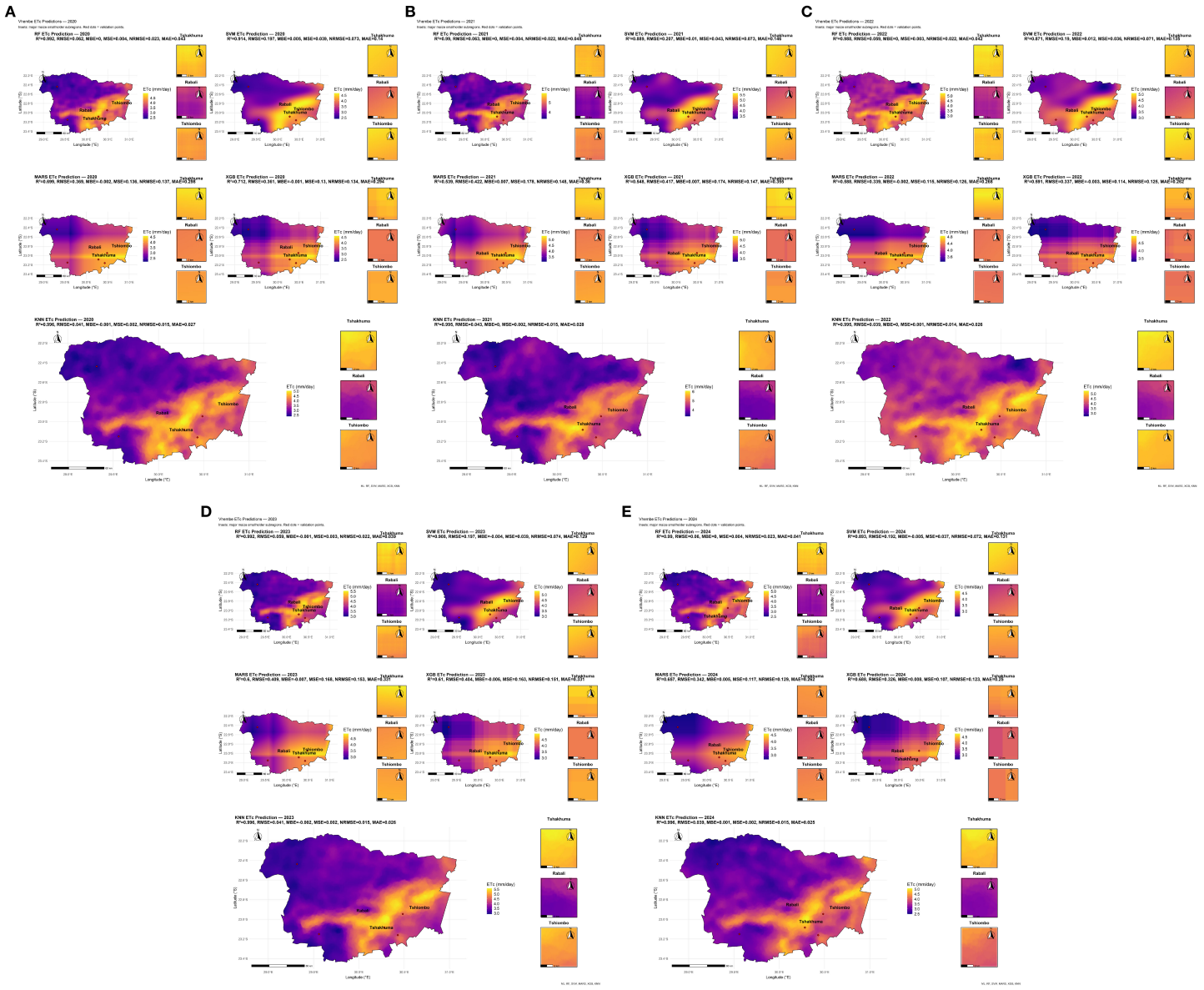

FIGURE 7
Spatial prediction of daily maize actual evapotranspiration (ET_c, mm/day) across Vhembe District for **(A)** 2020, **(B)** 2021, **(C)** 2022, **(D)** 2023, and **(E)** 2024, with performance comparison of five machine learning models: K-nearest neighbors (KNN), random forest (RF), support vector machine (SVM), multivariate adaptive regression splines (MARS), and extreme gradient boosting (XGB). The accompanying metrics panel table summarizes model evaluation statistics comparing ML predictions against FAO-56 benchmark values (ET_c,FAO-56) for independent test samples, including RMSE and coefficient of determination (R^2) values for each season and method.

10.3389/fagro.2025.1697188

advancement for smallholders facing increasingly complex water management challenge.

3.6 Machine learning-based uncertainty in maize evapotranspiration (ETc) predictions

Spatial patterns of daily maize ETc prediction uncertainty, represented by the 95% confidence interval (CI) width (mm/day) across Vhembe District from 2020 to 2024, reveal pronounced differences among five machine learning models: KNN, RF, SVM, MARS, and XGB [see Figures 8A–E]. KNN and RF consistently display the most localized and lowest uncertainty—evidenced by narrow CI widths—especially in agronomically critical subregions such as Tshakhuma, Rabali, and Tshombo, as shown in the inset panels. These spatially coherent zones of high predictive confidence align with areas of peak maize water demand and field-level variability, directly supporting precision irrigation management.

Conversely, SVM, MARS, and XGB models not only present broader CI widths and more heterogeneous uncertainty but also exhibit less spatial correspondence with agronomically important zones. The broader CIs reflect underlying model limitations in capturing fine-scale ET_c variability, as supported by lower R^2 and higher RMSE scores in the test set evaluation statistics. In regions where these models show wide confidence intervals, uncertainty is high, and field validation or adaptive management should take priority.

For smallholder farmers, actionable impact centers on using high-confidence map areas (from KNN and RF) to guide robust irrigation scheduling—optimizing timing and water use at site-specific scales. Conversely, fields residing in low-confidence (wide CI) areas signal locations where additional field measurements, contingency planning, or model refinement are essential to reduce risk and improve water management decisions. This dual approach enables both efficient irrigation in reliable zones and targeted monitoring in uncertain areas, improving farm resilience and yield consistency under dynamic climate conditions.

4 Discussion

The climatic context of the Vhembe District, characterized by erratic rainfall, recurrent droughts, and summer temperatures often exceeding 35°C, strongly conditions maize ET_c dynamics. Rainfall anomaly analyses revealed interannual variability with dry spells during reproductive stages, which directly heightened irrigation demand. These findings mirror broader observations in the Limpopo Basin and across southern Africa, where climate variability has consistently undermined smallholder crop productivity (Mavhungu et al., 2022; Sithole et al., 2023). Similar irrigation challenges have been reported in Mozambique and Zimbabwe, where unpredictable rainfall disrupted scheduling efficiency (Beekman et al., 2014; Moyo et al., 2017). The integration of Earth Observation (EO)-derived ETc monitoring thus provides a pathway to buffer maize production against such climatic uncertainty.

The actual crop evapotranspiration (ET_c) values observed in this study align well with existing literature for the Vhembe region, including the findings of Dzikiti et al. (2022) and FAO-56 guidelines for maize. This consistency reinforces the reliability of the models and approaches used, supporting their application for precision irrigation management in semi-arid smallholder contexts. Notably, the integration of the OPTRAM model with Sentinel-driven machine learning offers methodological novelty by demonstrating fine-scale ET_c estimation calibrated against *in-situ* probes. Few limted African studies have confirmed the suitability of OPTRAM for crop water monitoring in heterogeneous systems (Mananze and Pôças, 2019; Choukri et al., 2024), highlighting its potential to advance precision irrigation under climate stress.

The evaluation of machine learning models revealed that ensemble and neighborhood-based approaches—especially Random Forest and KNN—provided consistently superior predictive performance for maize ET_c ($R^2 > 0.99$, RMSE< 0.06 mm/day, and NRMSE often under 2%), decisively outperforming MARS and XGBoost, particularly in areas with complex, sharp soil–crop–climate interactions. Critically, the extremely low NRMSE values attained by RF and KNN underscore their practical utility for guiding irrigation machine scheduling, as NRMSE normalizes error across field conditions, giving smallholder farmers and automated systems a clear benchmark for precision water management both temporally and spatially. These results not only echo global research affirming the value of RF and KNN for non-linear water demand prediction (Stańczyk et al., 2023; Weitkamp and Karimi, 2023) but also reinforce that the ET_c thresholds and crop coefficients observed are directly relevant to smallholder irrigation decision-making (Negash et al., 2024).

Beyond predictive accuracy, the integration of EO and machine learning has direct livelihood implications. Studies in South Africa and Ethiopia confirm that smallholder irrigation reduces vulnerability to climatic shocks and enhances household welfare (Tesfay, 2021; Jiba et al., 2024). However, barriers remain related to infrastructure, data access, and governance (Van Averbeke et al., 2011; Bjornlund et al., 2017). Without targeted training and affordable delivery platforms, smallholder farmers may find it difficult to benefit from high-resolution irrigation advisories. Addressing these socio-economic dimensions is therefore crucial: the framework's outputs must be embedded into accessible tools such as SMS-based alerts or mobile applications linked with agricultural extension services. This would allow actionable irrigation guidance to reach farmers while minimizing costs and technical complexity. Looking forward, integrating affordable Internet of Things (IoT) soil moisture sensor networks with the proposed EO–AI framework could enable precise, real-time irrigation scheduling at the field level (Abdelmoneim et al., 2025). Leveraging widespread mobile connectivity and digital platforms, coupling such sensor data with regional advisory systems enhances scalability and operational reach (Benni, 2024). Moreover, adopting fintech innovations—such as mobile-based payments and microcredit platforms—could lower financial barriers by enabling smallholder farmers to invest in these precision irrigation technologies (Chen et al., 2024). This synergistic integration of

FIGURE 8
Spatial prediction of daily maize evapotranspiration (ETc, mm/day) across Vhembe District for **(A)** 2020, **(B)** 2021, **(C)** 2022, **(D)** 2023, and **(E)** 2024, with performance comparison of five machine learning models: K-nearest neighbors (KNN), random forest (RF), support vector machine (SVM), multivariate adaptive regression splines (MARS), and extreme gradient boosting (XGB).

10.3389/fagro.2025.1697188

IoT sensing, digital advisory services, and fintech-driven financial inclusion promises accessible, location-specific water management insights, reducing resource waste and fostering broader adoption of resilient irrigation practices among resource-limited farmers.

The scalability of the framework across sub-Saharan Africa is strengthened by its reliance on free-access Sentinel imagery, MODIS archives, and lightweight machine learning models. Comparable EO–AI approaches have been successfully applied in Ethiopia, Kenya, and Malawi for crop water monitoring under diverse agroecological conditions (Chipfupa and Wale, 2019; Dirwai et al., 2019; Hlatshwayo et al., 2023). More recent OPTRAM studies in Africa demonstrate transferability to other crops, including sorghum and sugarcane (Aringo et al., 2022; Negash et al., 2024), supporting the broader utility of the framework. However, successful operationalization will depend on integration into agricultural extension systems and water governance structures. Experiences from Zimbabwe and Mozambique highlight that irrigation interventions only succeed when embedded within supportive institutional and financial mechanisms (Beekman et al., 2014; Moyo et al., 2017). Thus, institutional alignment is as critical as technical accuracy in sustaining precision irrigation adoption in smallholder maize systems.

Several limitations warrant consideration. Model calibration relied on ARC probe data, which, while valuable, may not fully represent soil–crop heterogeneity across smallholder landscapes. Data gaps during extreme weather events remain challenging, even with radar–optical fusion. Furthermore, while RF and KNN proved robust, their dependence on balanced training datasets raises concerns about transferability to regions with limited calibration data (Matula et al., 2016; Weitkamp and Karimi, 2023). Future research should prioritize hybrid ensemble strategies combining OPTRAM, machine learning, and physically based models to leverage complementary strengths. Integrating these with low-cost IoT soil moisture sensors could further enable adaptive, real-time irrigation scheduling (Babaeian et al., 2019; Aringo et al., 2022). Equally important is policy support to strengthen water governance, capacity building, and farmer adoption pathways. By addressing these challenges, precision irrigation frameworks can evolve from localized case studies to transformative regional solutions for smallholder maize production under climate uncertainty.

A key limitation of this study is the assumption of a uniform maize planting date across the Vhembe District (10 November ± 5 days). This assumption simplifies crop-coefficient alignment but does not reflect the substantial planting-date variability typical of smallholder systems. In practice, planting dates vary by 2–4 weeks due to rainfall-onset uncertainty, delayed access to inputs and labour, and elevation-driven microclimatic differences (Nyagumbo et al., 2017). Farmers often wait for the first effective rainfall event (≥20 mm over three days), which can differ by 15–30 days between lowland and high-elevation areas (Mugiyo et al., 2021). Frost risk in the Soutpansberg (>800 m) also delays planting into late November or early December. These factors produce asynchronous phenology even among closely located fields (Moeletsi, 2017).

Such variability affects ETc estimation because crop water use is strongly phenology dependent. Late-planted maize shifts key growth stages, especially flowering and grain filling (BBCH 60–79), into hotter and sometimes drier periods (French et al., 2020). For instance, crops planted in mid-December often silk during late January, when daily temperatures >35°C are common, increasing actual ET_c relative to values predicted under a uniform planting assumption (Dong et al., 2021). NDVI time-series analysis in this study found that 15–20% of fields greened up 15–30 days later than assumed, with high-elevation fields showing consistent 10–14-day delays. Variation in NDVI-derived K_{cb} during the vegetative phase (CV = 18–25%) further indicates substantial phenological asynchrony. Together, these discrepancies likely contributed to localized ET_c deviations of 10–15% during peak-demand periods.

To address this limitation, future work should incorporate planting-date variability into the ET_c modelling workflow. A practical approach is to simulate ET_c under multiple planting windows that reflect typical smallholder behaviour. Table 4 provides an illustrative framework for early, standard, and late planting scenarios that can be used to generate probabilistic ET_c outputs.

Remote sensing–based phenology detection presents a promising pathway for integrating planting-date variability into ET_c modelling (Mkuhlani et al., 2019). Sentinel-2 time-series segmentation (e.g., double-logistic curve fitting or piecewise regression), red-edge band dynamics, and Sentinel-1 backscatter-derived canopy structure proxies can be used to detect field-level emergence dates (Liu et al., 2024). These dates could then be used to dynamically shift crop-coefficient curves using a simple temporal adjustment, K_c_adjusted(t) = Kc_standard(t − Δt_planting), where Δt_planting represents the planting delay relative to the baseline.

Incorporating farmer-reported planting dates through mobile platforms or extension agents' digital tools could further improve operational accuracy. Another promising direction is the adoption of growing degree day (GDD)–based phenology, which replaces calendar-day assumptions with temperature-driven development indicators, thereby harmonizing phenology across early- and late-planted fields.

Preliminary sensitivity analysis in this study (based on 150 fields with known planting dates from the 2021 season) indicates that incorporating planting-date variability could reduce peak-season ET_c RMSE by 10–15%, increase R^2 by 0.05–0.08 in heterogeneous terrain, and lower irrigation recommendation errors by 8–12 mm per season—equivalent to one to two irrigation events. These improvements would be most impactful in high-elevation areas, seasons with delayed rainfall onset, and among resource-constrained smallholder farmers whose planting schedules are more strongly affected by input and labour availability. Addressing this limitation will therefore enhance the robustness, transferability, and operational relevance of ETc-based irrigation advisory systems in complex smallholder landscapes.

5 Conclusion

This study presents a novel, scalable Earth Observation–AI framework that integrates multimodal earth obeservations, the

Optical Trapezoid Model (OPTRAM), and advanced machine learning algorithms to generate high-resolution, daily maize evapotranspiration (ET_c) maps in the Vhembe District of southern Africa. By fusing multimodal data sources to overcome persistent cloud cover and calibrating crop coefficients with maize phenological stages, the framework achieves robust ETc estimation validated against FAO Penman–Monteith reference methods and *in situ* soil moisture observations. Among the tested algorithms, Random Forest and k-Nearest Neighbors consistently outperformed alternatives, accurately capturing spatiotemporal variability in ET_c during critical growth phases and demonstrating practical relevance for precision irrigation scheduling.

The operational irrigation advisory frammework developed in this study translates complex EO and model outputs into actionable water-deficit alerts, offering smallholder farmers a low-cost, scalable, and climate-responsive decision-support tool. Beyond its application to maize, the framework is transferable to other crops and regions, providing a blueprint for enhancing irrigation efficiency and resilience in smallholder farming systems across sub-Saharan Africa.

Future research should prioritize three trajectories: (i) expanding field validation across diverse agroecological zones to ensure broader transferability, (ii) integrating hybrid approaches that combine OPTRAM, machine learning, and physically based crop models to improve robustness under extreme conditions, and (iii) embedding the framework into farmer-centric digital platforms linked with IoT soil moisture sensors to enable real-time adaptive irrigation. These steps will strengthen operational feasibility and scalability while aligning technological innovation with farmer needs and institutional structures.

Ultimately, this study contributes to advancing precision agriculture in Africa by demonstrating a viable pathway to enhance crop productivity, conserve scarce water resources, and improve smallholder resilience under increasing climatic uncertainty.

Data availability statement

The original contributions presented in the study are included in the article/Supplementary Material. Further inquiries can be directed to the corresponding author.

Author contributions

NS: Software, Writing – original draft, Formal Analysis, Writing – review & editing, Visualization, Data curation, Investigation, Validation, Methodology, Conceptualization. RS: Investigation, Resources, Writing – original draft, Funding acquisition, Visualization, Project administration, Conceptualization, Writing – review & editing, Data curation. ZD: Data curation, Writing – review & editing, Project administration, Investigation. AL: Formal Analysis, Visualization, Investigation, Writing – review & editing. AN: Writing – review & editing, Funding acquisition, Supervision, Resources, Formal Analysis, Conceptualization, Methodology.

Funding

The author(s) declared that financial support was received for this work and/or its publication. This research was supported by the János Bolyai Research Scholarship of the Hungarian Academy of Sciences. The research presented in the article was carried out within the framework of the Széchenyi Plan Plus program with the support of the RRF 2.3.1 21 2022 00008 project.

Conflict of interest

The authors declared that this work was conducted in the absence of any commercial or financial relationships that could be construed as a potential conflict of interest.

Generative AI statement

The author(s) declared that generative AI was not used in the creation of this manuscript.

Any alternative text (alt text) provided alongside figures in this article has been generated by Frontiers with the support of artificial intelligence and reasonable efforts have been made to ensure accuracy, including review by the authors wherever possible. If you identify any issues, please contact us.

Publisher's note

Supplementary material

The Supplementary Material for this article can be found online at: https://www.frontiersin.org/articles/10.3389/fagro.2025.1697188/full#supplementary-material

SUPPLEMENTARY TABLE 1
OPTRAM GEE Code Appendix (Seasonal Daily ETc).

SUPPLEMENTARY TABLE 2
Annual Spatial Mapping of ETc 95% Confidence Interval Widths (2020–2024), Vhembe District: Multi-Model Uncertainty Patterns, Maize Subregions (Insets), and Validation Sites.

SUPPLEMENTARY FIGURE 1
Spatial patterns of significant seasonal evapotranspiration (ETc) anomalies for maize in Vhembe District (2020 – 2024), highlighting only locations with $|z| \geq 1$.

References

Abdelmoneim, A. A., Kimaita, H. N., Al Kalaany, C. M., Derardja, B., Dragonetti, G., and Khadra, R. (2025). IoT sensing for advanced irrigation management: A systematic review of trends, challenges, and future prospects. *Sensors* 25, 2291. doi: 10.3390/s25072291

Aidoo, K., Browne Klutse, N. A., Asare, K., Botchway, C. G., and Fosuhene, S. (2021). Mapping evapotranspiration of agricultural areas in Ghana. *Sci. World J.* 2021, 1–7. doi: 10.1155/2021/8878631

Ali, I., Greifeneder, F., Stamenkovic, J., Neumann, M., and Notarnicola, C. (2015). Review of machine learning approaches for biomass and soil moisture retrievals from remote sensing data. *Remote Sens.* 7, 16398–16421. doi: 10.3390/rs71215841

Allen, R. G. (2000). *Crop evapotranspiration: guidelines for computing crop water requirements* (Rome: Food and Agriculture Organization of the United Nations).

Allen, R. G., Pereira, L. S., Raes, D., and Smith, M. (1998). *Crop evapotranspiration: Guidelines for computing crop water requirements (FAO Irrigation and Drainage Paper No. 56)* (Rome, Italy: Food and Agriculture Organization of the United Nations).

Ambrosone, M., Matese, A., Di Gennaro, S. F., Gioli, B., Tudoroiu, M., Genesio, L., et al. (2020). Retrieving soil moisture in rainfed and irrigated fields using Sentinel-2 observations and a modified OPTRAM approach. *Int. J. Appl. Earth Observation Geoinformation* 89, 102113. doi: 10.1016/j.jag.2020.102113

Aringo, M. Q., Martinez, C. G., Martinez, O. G., and Ella, V. B. (2022). Development of low-cost soil moisture monitoring system for efficient irrigation water management of upland crops. *IOP Conf. Ser.: Earth Environ. Sci.* 1038, 12029. doi: 10.1088/1755-1315/1038/1/012029

Aroonsrimorakot, S., and Laiphrakpam, M. (2023). Green supply chain management (GSCM) and circular economy (CE): A rapid review of their conceptual relationships: asia social issues. *Asia Social Issues* 17, e259742. doi: 10.48048/asi.2024.259742

Babaeian, E., Sidike, P., Newcomb, M. S., Maimaitijiang, M., White, S. A., Demieville, J., et al. (2019). A new optical remote sensing technique for high-resolution mapping of soil moisture. *Front. Big Data* 2. doi: 10.3389/fdata.2019.00037

Becaro Crioni, P. L., Hideo Teramoto, E., Favoreto Da Cunha, C., and Chang, H. K. (2025). Evaluation of the OPTRAM using sentinel-2 imagery to estimate soil moisture in urban environments. *Rev. Bras. Geog. Fis.* 18, 605–621. doi: 10.26848/rbgf.v18.1.p605-621

Beekman, W., Veldwisch, G. J., and Bolding, A. (2014). Identifying the potential for irrigation development in Mozambique: Capitalizing on the drivers behind farmer-led irrigation expansion. *Phys. Chem. Earth Parts A/B/C* 76–78, 54–63. doi: 10.1016/j.pce.2014.10.002

Benni, N. (2024). *Fintech innovation for smallholder agriculture* (Rome, Italy: FAO). doi: 10.4060/cc9117en

Bjornlund, H., Van Rooyen, A., and Stirzaker, R. (2017). Profitability and productivity barriers and opportunities in small-scale irrigation schemes. *Int. J. Water Resour. Dev.* 33, 690–704. doi: 10.1080/07900627.2016.1263552

Breiman, L. (2001). Random forests. *Mach. Learn.* 45, 5–32. doi: 10.1023/A:1010933404324

Cameira, M. D. R., and Santos Pereira, L. (2019). Innovation issues in water, agriculture and food. *Water* 11, 1230. doi: 10.3390/w11061230

Chen, X., He, G., and Li, Q. (2024). Can Fintech development improve the financial inclusion of village and township banks? Evidence from China. *Pacific-Basin Finance J.* 85, 102324. doi: 10.1016/j.pacfin.2024.102324

Chipfupa, U., and Wale, E. (2019). *Smallholder willingness to pay and preferences in the way irrigation water should be managed: a choice experiment application in KwaZulu-Natal, South Africa* (Pretoria, South Africa: WSA), 45. doi: 10.17159/wsa/2019.v45.i3.6735

Choukri, M., Laamrani, A., and Chehbouni, A. (2024). Use of optical and radar imagery for crop type classification in africa: A review. *Sensors* 24, 3618. doi: 10.3390/s24113618

Cortes, C., and Vapnik, V. (1995). Support-vector networks. *Mach. Learn* 20, 273–297. doi: 10.1007/BF00994018

Costa, T. S., Filgueiras, R., Dos Santos, R. A., and Cunha, F. F. D. (2023). Actual evapotranspiration by machine learning and remote sensing without the thermal spectrum. *PloS One* 18, e0285535. doi: 10.1371/journal.pone.0285535

Cover, T., and Hart, P. (1967). Nearest neighbor pattern classification. *IEEE Trans. Inform. Theory* 13, 21–27. doi: 10.1109/TIT.1967.1053964

Daryanto, S., Wang, L., and Jacinthe, P.-A. (2016). Global synthesis of drought effects on maize and wheat production. *PloS One* 11, e0156362. doi: 10.1371/journal.pone.0156362

Datta, S., Taghvaeian, S., Ochsner, T., Moriasi, D., Gowda, P., and Steiner, J. (2018). Performance assessment of five different soil moisture sensors under irrigated field conditions in oklahoma. *Sensors* 18, 3786. doi: 10.3390/s18113786

Dirwai, T. L., Senzanje, A., and Mudhara, M. (2019). Water governance impacts on water adequacy in smallholder irrigation schemes in KwaZulu-Natal province, South Africa. *Water Policy* 21, 127–146. doi: 10.2166/wp.2018.149

Dong, X., Guan, L., Zhang, P., Liu, X., Li, S., Fu, Z., et al. (2021). Responses of maize with different growth periods to heat stress around flowering and early grain filling. *Agric. For. Meteorology* 303, 108378. doi: 10.1016/j.agrformet.2021.108378

Dzikiti, S., Lotter, D., Mpandeli, S., and Nhamo, L. (2022). Assessing the energy and water balance dynamics of rain-fed rooibos tea crops (Aspalathus linearis) under changing Mediterranean climatic conditions. *Agric. Water Manage.* 274, 107944. doi: 10.1016/j.agwat.2022.107944

El-Beltagy, A., and Madkour, M. (2012). Impact of climate change on arid lands agriculture. *Agric. Food Secur* 1, 3. doi: 10.1186/2048-7010-1-3

Filgueiras, R., Chartuni Mantovani, E., Althoff, D., Balieiro Ribeiro, R., Peroni Venancio, L., and Argolo Dos Santos, R. (2019). DYNAMICS OF ACTUAL CROP EVAPOTRANSPIRATION BASED IN THE COMPARATIVE ANALYSIS OF SEBAL AND METRIC-EEFLUX. *R_I* 1, 72–80. doi: 10.15809/irriga.2019v1n1p72-80

Ford, T. W., McRoberts, D. B., Quiring, S. M., and Hall, R. E. (2015). On the utility of in *situ* soil moisture observations for flash drought early warning in Oklahoma, USA. *Geophysical Res. Lett.* 42, 9790–9798. doi: 10.1002/2015GL066600

Ford, T. W., and Quiring, S. M. (2019). Comparison of contemporary in situ, model, and satellite remote sensing soil moisture with a focus on drought monitoring. *Water Resour. Res.* 55, 1565–1582. doi: 10.1029/2018WR024039

French, A. N., Hunsaker, D. J., Sanchez, C. A., Saber, M., Gonzalez, J. R., and Anderson, R. (2020). Satellite-based NDVI crop coefficients and evapotranspiration with eddy covariance validation for multiple durum wheat fields in the US Southwest. *Agric. Water Manage.* 239, 106266. doi: 10.1016/j.agwat.2020.106266

Friedman, J. H. (1991). Multivariate adaptive regression splines. *Ann. Statist.* 19, 1–67. doi: 10.1214/aos/1176347963

Friedman, J. H. (2001). Greedy function approximation: A gradient boosting machine. *Ann. Statist* 29, 1189–1232. doi: 10.1214/aos/1013203451

Hlatshwayo, S. I., Ngidi, M. S. C., Ojo, T. O., Modi, A. T., Mabhaudhi, T., and Slotow, R. (2023). The determinants of crop productivity and its effect on food and nutrition security in rural communities of South Africa. *Front. Sustain. Food Syst.* 7. doi: 10.3389/fsufs.2023.1091333

Ibrahim, M. M., El-Baroudy, A. A., and Taha, A. M. (2016). Irrigation and fertigation scheduling under drip irrigation for maize crop in sandy soil. *Int. Agrophysics* 30, 47–55. doi: 10.1515/intag-2015-0071

Jiba, P., Obi, A., Mdoda, L., and Mzuyanda, C. (2024). The impact of smallholder irrigation scheme on household welfare in farm-managed irrigation scheme communities in the eastern cape province, South Africa. *S Afr. Jnl. Agric. Ext.* 52, 48–72. doi: 10.17159/2413-3221/2024/v52n1a13953

Kolady, D. E., van der Sluis, E., Uddin, M. M., and Deutz, A. P. (2021). Determinants of adoption and adoption intensity of precision agriculture technologies: evidence from South Dakota. *Precis. Agric.* 22, 689–710. doi: 10.1007/s11119-020-09750-2

Legates, D. R., and McCabe, G. J. (1999). Evaluating the use of "goodness-of-fit" Measures in hydrologic and hydroclimatic model validation. *Water Resour. Res.* 35, 233–241. doi: 10.1029/1998WR900018

Liu, X., Forkel, M., and Kranz, J. (2024). Investigating the association of seasonal dynamics in GEDI canopy cover profiles and sentinel-1 backscatter in temperate forests. IEEE geosci. *Remote Sens. Lett.* 21, 1–5. doi: 10.1109/LGRS.2024.3443525

Mananze, S., and Pôças, I. (2019). Agricultural drought monitoring based on soil moisture derived from the optical trapezoid model in Mozambique. *J. Appl. Rem. Sens.* 13, 1. doi: 10.1117/1.JRS.13.024519

Maponya, P. (2021). Opportunities and constraints faced by smallholder farmers in the vhembe district, limpopo province in South Africa. *Circ.Econ.Sust* 1, 1387–1400. doi: 10.1007/s43615-021-00028-x

Matasane, C., and Kahn, M. (2025). "Assessing renewable energy potential in vhembe district using GIS and remote sensing," in *International Conference on Trends and Innovations in Management, Engineering, Sciences and Humanities (ICTIMESH-24)*, (Dubai: International Journal of Innovative Research in Engineering & Multidisciplinary Physical Sciences), ICTIMESH-24 Dubai. doi: 10.37082/IJIRMPS.ICTIMESH-24-Dubai.6

Matula, S., Báťková, K., and Legese, W. (2016). Laboratory performance of five selected soil moisture sensors applying factory and own calibration equations for two soil media of different bulk density and salinity levels. *Sensors* 16, 1912. doi: 10.3390/s16111912

Mauder, M., Foken, T., Aubinet, M., and Ibrom, A. (2021). "Eddy-covariance measurements," in *Springer Handbook of Atmospheric Measurements*. Ed. T. Foken (Springer International Publishing, Cham), 1473–1504. doi: 10.1007/978-3-030-52171-4_55

Mavhungu, T. J., Nesamvuni, A. E., Tshikolomo, K. A., Mpandeli, N. S., and Van Niekerk, J. (2022). Productivity and profitability of sweet potato (ipomoea batatas l.), dry bean (Phaseolus Vulgaris) and maize (Zea mays l.) as selected field crops in irrigated smallholder agricultural enterprises (ISAEs) in Vhembe District, Limpopo Province, South Africa. *TSSJ* 29, 683–699. doi: 10.47577/tssj.v29i1.5932

Mentaschi, L., Besio, G., Cassola, F., and Mazzino, A. (2013). Problems in RMSE-based wave model validations. *Ocean Model.* 72, 53–58. doi: 10.1016/j.ocemod.2013.08.003

Mkuhlani, S., Mupangwa, W., and Nyagumbo, I. (2019). "Maize Yields in Varying Rainfall Regimes and Cropping Systems Across Southern Africa: A Modelling Assessment," in *University Initiatives in Climate Change Mitigation and Adaptation*. Eds. W. Leal Filho and R. Leal-Arcas (Springer International Publishing, Cham), 203–228. doi: 10.1007/978-3-319-89590-1_12

Moeletsi, M. E. (2017). Mapping of maize growing period over the free state province of South Africa: heat units approach. *Adv. Meteorology* 2017, 1–11. doi: 10.1155/2017/7164068

Moeletsi, M. E., Myeni, L., Kaempffer, L. C., Vermaak, D., De Nysschen, G., Henningse, C., et al. (2022). Climate dataset for South Africa by the agricultural research council. *Data* 7, 117. doi: 10.3390/data7080117

Mohamadzadeh, N., Sadeghi, M., Vergopolan, N., Liang, L., Bandara, U., Altare, C., et al. (2025). Landcover-specific calibration of the optical trapezoid model (OPTRAM) for soil moisture monitoring in the Central Valley, California. *Front. Remote Sens.* 6. doi: 10.3389/frsen.2025.1519420

Moriasi, D. N., Arnold, J. G., Liew, M. W. V., Bingner, R. L., Harmel, R. D., and Veith, T. L. (2007). Model evaluation guidelines for systematic quantification of accuracy in watershed simulations. *Trans. ASABE* 50, 885–900. doi: 10.13031/2013.23153

Moyo, M., Van Rooyen, A., Moyo, M., Chivenge, P., and Bjornlund, H. (2017). Irrigation development in Zimbabwe: understanding productivity barriers and opportunities at Mkoba and Silalatshani irrigation schemes. *Int. J. Water Resour. Dev.* 33, 740–754. doi: 10.1080/07900627.2016.1175339

Mugiyo, H., Mhizha, T., Chimonyo,, Vimbayi., G. P., and Mabhaudhi, T. (2021). Investigation of the optimum planting dates for maize varieties using a hybrid approach: A case of Hwedza, Zimbabwe. *Heliyon* 7, e06109. doi: 10.1016/j.heliyon.2021.e06109

Nagy, A., Kiss, N.É., Buday-Bódi, E., Magyar, T., Cavazza, F., Gentile, S. L., et al. (2024). Precision estimation of crop coefficient for maize cultivation using high-resolution satellite imagery to enhance evapotranspiration assessment in agriculture. *Plants* 13, 1212. doi: 10.3390/plants13091212

Negash, T. W., Tefera, A. T., and Bayisa, G. D. (2024). Maize (Zea mays L. 1753) evapotranspiration ando crop coefficient in semi-arid region of Ethipia. *IJAm* 29, 55–63. doi: 10.36253/ijam-2777

Nuwarinda, H., Ramoelo, A., and Adelabu, S. A. (2022). Assessing natural resource change drivers in Vhembe Biosphere and surroundings. *JSM Environ. Sci. Ecol.* 10, 1083 doi: 10.47739/2333-7141/1083

Nyagumbo, I., Mkuhlani, S., Mupangwa, W., and Rodriguez, D. (2017). Planting date and yield benefits from conservation agriculture practices across Southern Africa. *Agric. Syst.* 150, 21–33. doi: 10.1016/j.agsy.2016.09.016

Pareeth, S., and Karimi, P. (2023). Evapotranspiration estimation using Surface Energy Balance Model and medium resolution satellite data: An operational approach for continuous monitoring. *Sci. Rep.* 13, 12026. doi: 10.1038/s41598-023-38563-2

Quintana-Molina, J. R., Sánchez-Cohen, I., Jiménez-Jiménez, S. I., Marcial-Pablo, M. D. J., Trejo-Calzada, R., and Quintana-Molina, E. (2023). Calibration of volumetric soil moisture using Landsat-8 and Sentinel-2 satellite imagery by Google Earth Engine. *Rev. Teledetec* 60, 21–38. doi: 10.4995/raet.2023.19368

Reusser, D. E., Blume, T., Schaefli, B., and Zehe, E. (2009). Analysing the temporal dynamics of model performance for hydrological models. *Hydrol. Earth Syst. Sci.* 13, 999–1018. doi: 10.5194/hess-13-999-2009

Sanchez, O. R., Repetto, M., Carrega, A., and Bolla, R. (2021). "Evaluating ML-based DDoS detection with grid search hyperparameter optimization," in *2021 IEEE 7th International Conference on Network Softwarization (NetSoft)*, Tokyo, Japan. IEEE 402–408 (IEEE). doi: 10.1109/NetSoft51509.2021.9492633

Semenya, S. S., and Potgieter, M. J. (2014). Bapedi traditional healers in the Limpopo Province, South Africa: Their socio-cultural profile and traditional healing practice. *J. Ethnobiology Ethnomedicine* 10, 4. doi: 10.1186/1746-4269-10-4

Shikwambana, S., Malaza, N., and Shale, K. (2021). Impacts of rainfall and temperature changes on smallholder agriculture in the limpopo province, South Africa. *Water* 13, 2872. doi: 10.3390/w13202872

Siphiwe, N. G., Magyar, T., Tamás, J., and Nagy, A. (2024). Modelling soil moisture content with hydrus 2D in a continental climate for effective maize irrigation planning. *Agriculture* 14, 1340. doi: 10.3390/agriculture14081340

Sithole, Z., Siwela, M., Ojo, T. O., Hlatshwayo, S. I., Kajombo, R. J., and Ngidi, M. S. C. (2023). Contribution of fruits and vegetables to the household food security situation of rural households in limpopo. *Nutrients* 15, 2539. doi: 10.3390/nu15112539

Stańczyk, T., Kasperska-Wołowicz, W., Szatyłowicz, J., Gnatowski, T., and Papierowska, E. (2023). Surface soil moisture determination of irrigated and drained agricultural lands with the OPTRAM method and sentinel-2 observations. *Remote Sens.* 15, 5576. doi: 10.3390/rs15235576

Tesfay, M. G. (2021). Impact of irrigated agriculture on welfare of farm households in northern Ethiopia: panel data evidence*. *Irrigation Drainage* 70, 306–320. doi: 10.1002/ird.2545

Trout, T. J., and DeJonge, K. C. (2021). Evapotranspiration and water stress coefficient for deficit-irrigated maize. *J. Irrig. Drain Eng.* 147, 04021044. doi: 10.1061/(ASCE)IR.1943-4774.0001600

Van Averbeke, W., Denison, J., and Mnkeni, P. (2011). Smallholder irrigation schemes in South Africa: A review of knowledge generated by the Water Research Commission. *WSA* 37, 797–808. doi: 10.4314/wsa.v37i5.17

Weitkamp, T., and Karimi, P. (2023). Evaluating the effect of training data size and composition on the accuracy of smallholder irrigated agriculture mapping in Mozambique using remote sensing and machine learning algorithms. *Remote Sens.* 15, 3017. doi: 10.3390/rs15123017

Willmott, C., and Matsuura, K. (2005). Advantages of the mean absolute error (MAE) over the root mean square error (RMSE) in assessing average model performance. *Clim. Res.* 30, 79–82. doi: 10.3354/cr030079

Zhu, J.-J., Yang, M., and Ren, Z. J. (2023). Machine learning in environmental research: common pitfalls and best practices. *Environ. Sci. Technol.* 57, 17671–17689. doi: 10.1021/acs.est.3c00026